Inorganic Chemistry

Article

pubs.acs.org/IC

Alkali Metal Directed Assembly of Heterometallic V^V/M (M = Na, K, Cs) Coordination Polymers: Structures, Topological Analysis, and Oxidation Catalytic Properties

Samik Gupta,[†] Marina V. Kirillova,[†] M. Fátima C. Guedes da Silva,*[,†,‡] Armando J. L. Pombeiro,*[,†] and Alexander M. Kirillov*[,†]

[†]Centro de Química Estrutural, Complexo I, Instituto Superior Técnico, Technical University of Lisbon, Av. Rovisco Pais, 1049-001, Lisbon, Portugal

[‡]Universidade Lusófona de Humanidades e Tecnologias, ULHT, Lisbon, Av. do Campo Grande, 376, 1749-024, Lisbon, Portugal

Supporting Information

ABSTRACT: The reactions of $[VO(acac)_2]$ with bis(salicylaldehyde)-oxaloyldihydrazone (H_4L) and an alkali metal carbonate M_2CO_3 (M = K, Na, Cs), in EtOH/H_2O medium upon reflux, resulted in the generation of three new heterometallic V^V/M materials, namely the 1D $[(VO_2)_2(\mu_4\text{-}L)\{Na_2(\mu\text{-}H_2O)_2(H_2O)_2\}]_n$ (**1**), 2D $[\{V(\mu\text{-}O)_2\}_2(\mu_4\text{-}L)\{K_2(\mu\text{-}H_2O)_2(H_2O)_2\}]_n$ (**2**), and 3D $[\{V(\mu\text{-}O)(\mu_3\text{-}O)\}_2(\mu_8\text{-}L)\{Cs_2(\mu\text{-}H_2O)_2(H_2O)_2\}]_n$ (**3**) coordination polymers. They were isolated as air-stable solids and fully characterized by IR, UV–vis, ^1H, and ^{51}V NMR spectroscopy, ESI–MS(±), elemental, thermal, and single-crystal X-ray diffraction analyses, the latter showing that **1**–**3** are constructed from the resembling $[(VO_2)_2(\mu_{4/8}\text{-}L)]^{2-}$ blocks assembled by the differently bound aqua-metal $[M_2(\mu\text{-}H_2O)_2(H_2O)_2]^{2+}$ moieties (M = Na, K, Cs). The main distinctive features of **1**–**3** arise from the different coordination numbers of Na (5), K (7), and Cs (9) atoms, thus increasing the complexity of the resulting networks from the ladder-like 1D chains in **1** to double 2D layers in **2**, and layer-pillared 3D framework in **3**. The topological analysis of **2** disclosed a uninodal 4-connected underlying net with a rare **kgm** [Shubnikov plane net (3.6.3.6)/kagome pattern] topology, while **3** features a trinodal 4,7,8-connected underlying net with an unprecedented topology. Compounds **1**–**3** also show solubility in water ($S_{25\ °C} \approx 4$–7 mg mL^{-1}) and were applied as efficient precatalysts for the homogeneous oxidation of cyclohexane by aqueous H_2O_2, under mild conditions (50 °C) in MeCN/H_2O medium and in the presence of an acid promoter. Total yields (based on substrate) of cyclohexanol and cyclohexanone up to 36% and turnover numbers (TONs) up to 5700 were achieved.

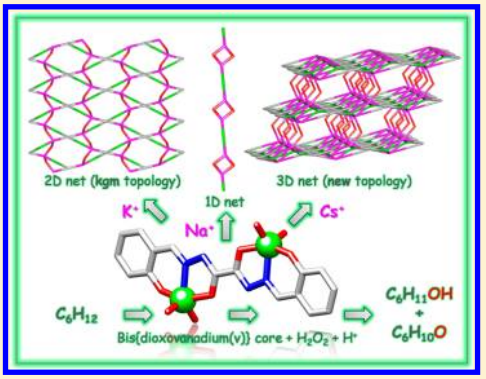

INTRODUCTION

Within the sweeping development of the research on coordination polymers in recent years,[1,2] the design of new vanadium containing materials with attractive functional properties[3] is primarily associated with the unique redox, catalytic, and coordinative versatility of the vanadium ions[4] in such metal–organic networks. In particular, the search for novel organic building blocks and vanadium-based nodes to generate coordination polymers with desired properties is a promising research direction, which can lead to new materials with unusual structural, topological, and functional characteristics.

In this regard, we have focused our attention on the oxaloyldihydrazone derivative [H_4L, bis(salicylaldehyde)-oxaloyldihydrazone, Scheme 1], which, in spite of possessing up to eight potential N,O-coordination sites and an ability to bind vanadium[5] and other metal centers,[6,7] has not yet been applied as a building block toward the design of coordination polymers, as confirmed by a search of the Cambridge Structural Database.[7] From the other side, the common s-block metal centers are known as versatile nodes[8] to compose various V-based secondary building units (SBUs) into coordination networks.[7] Bearing these points in mind, the first objective of the present study was to probe the complexation of vanadium ions with H_4L, followed by assembling the resulting SBUs into heterometallic V/M coordination polymers driven by different alkali metals (M = Na, K, Cs). Moreover, given the recognized application of various vanadium compounds with N,O-ligands in oxidation catalysis[9] and our interest toward the development of efficient V-based catalytic systems for the mild oxidative

Scheme 1. Structural Formula of H_4L

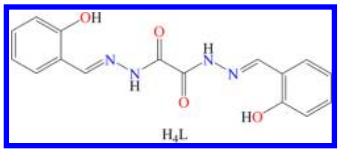

Received: March 26, 2013

 © XXXX American Chemical Society dx.doi.org/10.1021/ic400743h | *Inorg. Chem.* XXXX, XXX, XXX–XXX

Scheme 2. Simplified Representation of the Synthesis and Structural Formulae of 1−3[a]

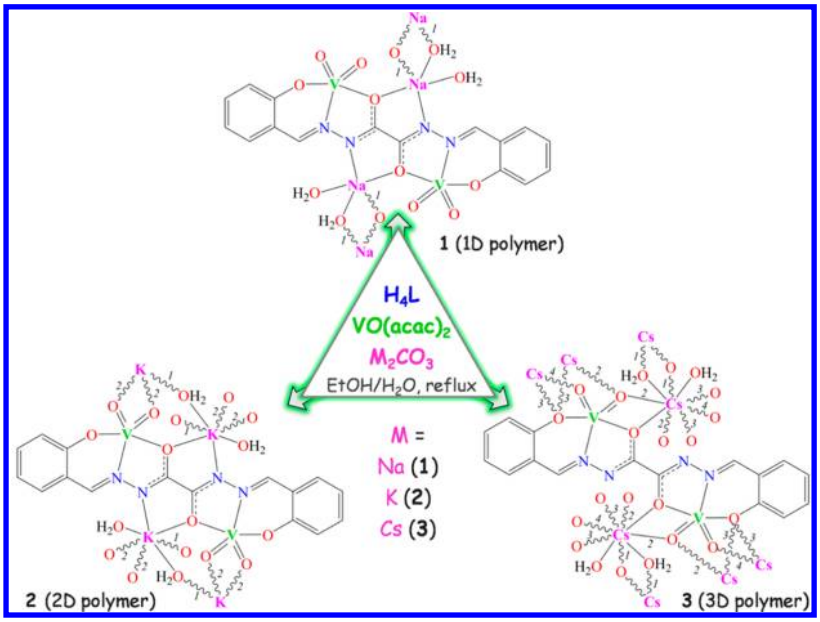

[a]Numbers *1*, *2*, *3*, and *4* correspond to extensions of polymeric motifs.

functionalization of alkanes,[10,11] the second objective of the current work consisted in exploring such a catalytic direction, namely by testing the obtained coordination polymers as precatalysts in the oxidation of cyclohexane as a model substrate.

Hence, we describe herein the synthesis, full characterization, structural features, and catalytic application of three new heterometallic V^v/Na (**1**), V^v/K (**2**), and V^v/Cs (**3**) coordination polymers. Apart from revealing an interesting example of periodicity wherein the network complexity increases from Na (1D) to K (2D) and Cs (3D), the obtained compounds constitute the first coordination polymers of any metal that derived from the oxaloyldihydrazone H_4L building block.[7] Furthermore, the present study shows that **1**−**3** are rare examples of aqua-soluble coordination polymers,[12,13] which also act as efficient precatalysts for the homogeneous oxidation of cyclohexane, by H_2O_2 in MeCN/H_2O medium and under mild conditions, to give cyclohexanol and cyclohexanone.

RESULTS AND DISCUSSION

Synthesis and Characterization. Aiming at the synthesis of new heterometallic V/M (M = Na, K, Cs) coordination polymers supported by multifunctional N,O-ligands, we selected an oxaloyldihydrazone derivative H_4L as a main building block, since its application in coordination chemistry is still very limited.[5−7] Hence, treatment of H_4L with $[VO(acac)_2]$ in ethanol under reflux in air, followed by the addition of an aqueous solution of alkali metal carbonate M_2CO_3, gave rise to the series of coordination polymers $[(VO_2)_2(\mu_4\text{-L})\{Na_2(\mu\text{-}H_2O)_2(H_2O)_2\}]_n$ (**1**), $[\{V(\mu\text{-}O)_2\}_2(\mu_4\text{-L})\{K_2(\mu\text{-}H_2O)_2(H_2O)_2\}]_n$ (**2**), and $[\{V(\mu\text{-O})(\mu_3\text{-O})\}_2(\mu_8\text{-L})\{Cs_2(\mu\text{-}H_2O)_2(H_2O)_2\}]_n$ (**3**) (Scheme 2). The observed herein oxidation of the vanadium(IV) precursor $[VO(acac)_2]$ to give the vanadium(V) products **1**−**3** is driven by the presence of dioxygen, moist EtOH, and reflux conditions.[4e,14a,b] In fact, $[VO(acac)_2]$ is known to undergo the oxidation to V^V species in the presence of dioxygen,[14a] opening up an entry to various vanadium(V) derivatives that also include those with the related N,O-ligands.[4,5] Although all the compounds **1**−**3** bear resembling $[(VO_2)_2(L)]^{2-}$ units, the main distinctive features arise from different coordination environments around Na, K, and Cs atoms. In fact, the coordination number of M^+ rises from 5 (Na) to 7 (K) and 9 (Cs) on going from a lighter to a heavier alkali metal ion. As a consequence, the complexity of the resulting network increases from 1D chains in **1** to 2D layers in **2**, and 3D framework in **3**. A key role in defining the dimensionality of the obtained polymers is thus played by the type of alkali metal. The new products **1**−**3** were isolated as yellow air-stable solids in good yields (72−76% based on H_4L) and fully characterized by IR, ^1H and ^{51}V NMR, and UV−vis spectroscopy, ESI-MS(±), elemental, thermal, and single-crystal X-ray diffraction analysis.

The IR spectra of **1**−**3** show comparable features due to the presence of similar $[(VO_2)_2(L)]^{2-}$ units and hydrated alkali metal ions. Hence, very strong bands in the 3700−3000 cm^{-1} region with maxima at 3430−3445 cm^{-1} are assigned to $\nu(H_2O)$ vibrations, their broad character being associated with multiple hydrogen bonding interactions.[14c] Other characteristic $\nu(C{=}O)$ and $\nu(C{=}N)$ vibrations appear as intense bands with maxima at 1607−1608 and 1547−1548 cm^{-1}, respectively.[5] As expected, these bands in **1**−**3** are shifted in comparison with those of H_4L [1692 $\nu(C{=}O)$ and 1595 $\nu(C{=}N)$ cm^{-1}]. The detection of strong and broad $\nu(V{=}O)$ vibrations centered at 915 (**1**), 913 (**2**), and 921 (**3**) cm^{-1} supports the presence of the *cis*-VO_2 groups in all compounds.[5] In addition, the $\nu(V{=}O)$ bands in **2** and **3** possess shoulders at 875−872 cm^{-1} that are presumably associated with the bridging μ_2- or μ_3-O modes of oxido ligands, as a result of additional binding to K or Cs atoms. The solution UV−vis spectra of **1**−**3** show broad absorptions with maxima at 324−325 and 409−414 nm that are assigned to ligand-to-metal charge transfer.[15a] The solution ^1H NMR spectra of **1**−**3** are rather similar and reveal expected signals due to aromatic C−H or C(H)=N protons, which occur as two multiplets at δ 6.86−6.98 and 7.44−7.62 or singlets at δ 8.88−8.91, respectively.[15b] The absence of signals corresponding to the NH and OH protons confirms the

dx.doi.org/10.1021/ic400743h | *Inorg. Chem.* XXXX, XXX, XXX−XXX

deprotonated L(4−) form of the ligand. The ^{51}V NMR spectra of **1**−**3** in aqueous CD_3CN are also similar, showing one resonance at δ −538 (Figure S1, Supporting Information).

A significant feature of **1**−**3** consists in their water solubility ($S_{25°C} \approx 4$−7 mg mL^{-1}) because hydrosoluble coordination polymers are still rare,[12,13] in spite of possessing rather high potential for biological[16] or catalytic[12] applications in aqueous media. Although the solubility of **1**−**3** in H_2O is eventually associated with their partial dissociation into ionic species via decoordination of alkali metal ions, the ESI-MS(+) spectra of **1**−**3** also reveal the presence of moieties that resemble those of molecular ions of the repeating units. Hence, the $[(VO_2)_2(L)Na_2 + Na]^+$ (m/z = 557) and $[(VO_2)_2(L)K_2(H_2O)_2 + H]^+$ (m/z = 604) fragments are detected as the most intense peaks (100% relative intensity) in the ESI-MS(+) spectra of **1** and **2**. The related $[(VO_2)_2(L)Cs_2 + Cs]^+$ (m/z = 886) and $[(VO_2)_2(L)Cs_2 + H]^+$ (m/z = 755) fragments are also observed in the respective spectrum of **3**, although of low intensity due to a poor fragmentation in the positive mode. Other signals detected in ESI-MS(+) of **1** and **2** correspond to $[(VO_2)_2(L)Na_2(H_2O)_4 + VO_2]^+$ (m/z = 690), $[(VO_2)_2(L)Na_2(H_2O)_4 + H_2O + H]^+$ (m/z = 625), $[(VO_2)_2(L)K_2(H_2O)_3 + K]^+$ (m/z = 660), and $[(VO_2)(L)K_2 + 2H]^+$ (m/z = 485) fragments. The ESI−MS(−) plots further confirmed the formulations of **1**−**3**, revealing the characteristic $[(VO_2)_2(L)M]^-$ (m/z = 511, 527, and 621 in **1**−**3**, respectively), $[(VO_2)_2(L) + H]^-$ (m/z = 489), and $[(VO_2)_2(L)]^{2-}$ (m/z = 244) fragments with expected isotopic distribution patterns.

The differential thermal analyses of **1**−**3** show three to five thermal effects. The endothermic effects in the 30−130 (**1**), 40−170 (**2**), or 40−160 (**3**) °C temperature range correspond to removal of four (in **1**) or two (in **2**, **3**) water ligands. Interestingly, the elimination of the two remaining water molecules in **2** and **3** only begins at 230 °C, supporting a stronger binding of μ-H_2O ligands in these compounds. The subsequent exothermic effects in the 260−550 (**1**), 230−520 (**2**), or 230−400 (**3**) °C temperature intervals are mainly associated to the multistep decomposition of L, resulting in MVO_3 (M = Na, K, Cs) as major decomposition products.

X-ray Crystal Structures. The crystal structures of **1**−**3** are composed of one vanadium(V) atom, one alkali metal atom, half of L(4−) moiety, two oxido ligands, and two aqua ligands per asymmetric unit. These are arranged into resembling $[(VO_2)_2(L)]^{2-}$ blocks that are interconnected through the differently bound aqua-metal $[M_2(\mu\text{-}H_2O)_2(H_2O)_2]^{2+}$ moieties (M = Na, K, Cs), resulting in the formation of distinct heterometallic 1D, 2D, and 3D metal−organic networks, respectively.

*$[(VO_2)_2(\mu_4\text{-}L)\{Na_2(\mu\text{-}H_2O)_2(H_2O)_2\}]_n$ (**1**).* In **1**, the $[(VO_2)_2(\mu_4\text{-}L)]^{2-}$ blocks consist of the two symmetry related V1 atoms, two pairs of terminal oxido O3 and O4 moieties, and one tetradeprotonated μ_4-L(4−) ligand in transoid conformation (Figure 1a). The five-coordinate V1 atoms adopt distorted $\{VNO_4\}$ square-pyramidal environments (τ_5 = 0.21), filled by the N1, O1, and μ-O2 atoms of μ_4-L and the O4 oxido ligand in basal positions [V1−N1 2.131(2), V1−O1 1.8821(16), V1−O2 1.9993(16), V1−O4 1.6434(17) Å], while the O3 oxido ligand is located in the apical site [V1−O3 1.6188(18) Å]. Within the $[Na_2(\mu\text{-}H_2O)_2(H_2O)_2]^{2+}$ moieties, the Na1 atoms are five-coordinate and also possess distorted $\{NaNO_4\}$ geometries that are better described as square-pyramidal (τ_5 = 0.18). These are filled by the μ-O2 and N2 atoms of μ_4-L, and the O5 and μ-O6^{ii} atoms of aqua ligands in equatorial sites

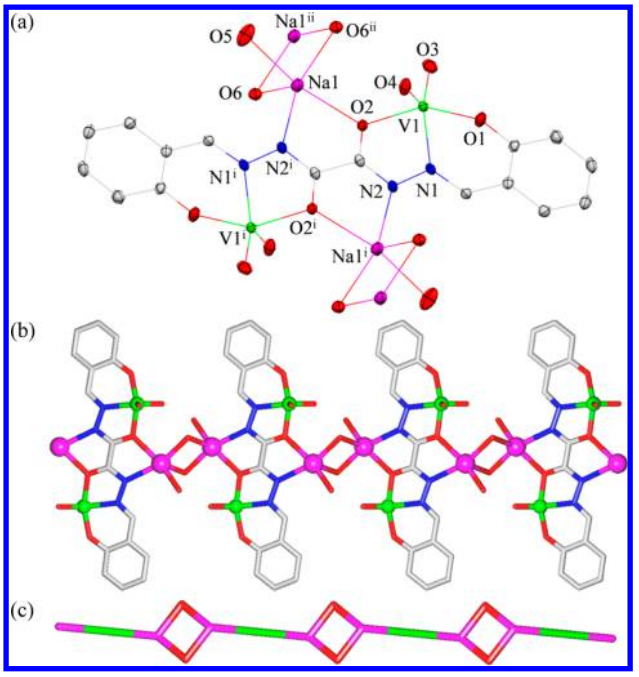

Figure 1. Structural fragments of **1** showing (a) ellipsoid plot (50% probability) with partial atom labeling scheme, (b) ladder-like 1D chain (view along the *a* axis), (c) topological representation of the underlying 1D network. Further details: (a, b) H atoms are omitted for clarity, color codes: V (green), Na (magenta), N (blue), O (red), and C (gray); (c) 3-connected Na nodes (magenta), centroids of the 2-connected $[(VO_2)_2(\mu_4\text{-}L)]^{2-}$ (green) and μ-H_2O (red) linkers. Selected distances (Å): V1−N1 2.131(2), V1−O1 1.8821(16), V1−O2 1.9993(16), V1−O3 1.6188(18), V1−O4 1.6434(17), Na1^i−N2 2.419(2), Na1−O2 2.3529(17), Na1−O5 2.270(2), Na1−O6 2.3421(19), Na1^{ii}−O6 2.3595(19), V1···Na1 3.856(1), Na1···Na1^{ii} 3.355(1), Na1···Na1^i 6.217(2), V1···V1^i 7.0720(5). Symmetry codes: (i) 1 − *x*, 1 − *y*, −*z*; (ii) 1 − *x*, 1 − *y*, 1 − *z*, (iii) *x*, 1 + *y*, *z*; (iv) 1 + *x*, *y*, *z*.

[Na1−O2 2.352(2), Na1−N2^i 2.419(2), Na1−O5 2.270(2), Na1−O6^{ii} 2.358(2) Å], whereas an axial site is taken by the second μ-O6 atom of μ-H_2O ligand [Na1−O6 2.3595(19) Å]. Hence, each of the oxaloyldihydrazone ligands acts in a μ_4-bridging mode, simultaneously binding two V1 and two Na1 atoms with a $\{N_4O_4\}$ donor set and resulting in the formation of almost planar tetrametallic $[V_2Na_2(\mu_4\text{-}L)]$ fragments with the metal separations of 3.856(1) [V1···Na1], 6.217(2) [Na1···Na1^i], and 7.0720(5) Å [V1···V1^i]. Together with the additional oxido (O3, O4) and aqua (O5, O6) ligands, these generate more complex $[(VO_2)_2(\mu_4\text{-}L)\{Na_2(\mu\text{-}H_2O)_2(H_2O)_2\}]$ units that are mutually interconnected through μ-H_2O (O6) linkers into infinite ladder-like 1D metal−organic chains (Figures 1b,c). Multiple interchain H-bonds [O5−H5B···O1^{iii} 2.887(2), O6−H6B···O3^{iv} 2.764(2) Å] provide further extension of the 1D coordination network into a 3D supramolecular assembly.

*$[\{V(\mu\text{-}O)_2\}_2(\mu_4\text{-}L)\{K_2(\mu\text{-}H_2O)_2(H_2O)_2\}]_n$ (**2**).* As in the case of **1**, the structure of **2** (Figure 2a) also bears the resembling $[(VO_2)_2(\mu_4\text{-}L)]^{2-}$ blocks, which, therefore, are not discussed further in detail. However, the main distinctive feature of **2** consists in different and more complex coordination behavior of the K1 atoms, namely concerning their interactions with the μ-oxido (O3, O4) and μ-H_2O (O5) ligands. Hence, the symmetry generated K1 atoms (two per formula unit) adopt seven-coordinate $\{KNO_6\}$ environments, which are occupied

dx.doi.org/10.1021/ic400743h | *Inorg. Chem.* XXXX, XXX, XXX−XXX

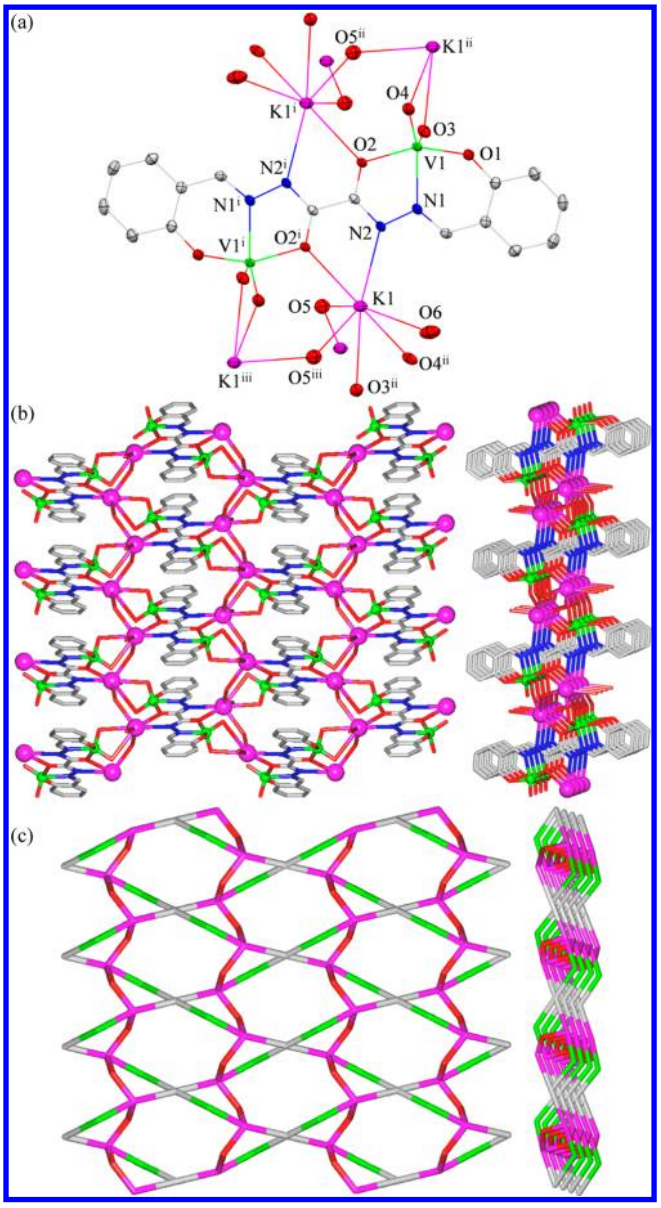

Figure 2. Structural fragments of **2** showing (a) ellipsoid plot (50% probability) with partial atom labeling scheme, (b) front (left) and side (right) views of the metal−organic double 2D layer assembled from helical 1D ribbons, (c) topological representation of the underlying uninodal 4-connected 2D net with the **kgm** [Shubnikov plane net (3.6.3.6)/kagome pattern] topology and the point symbol of $(3^2.6^2.7^2)$. Further details: (a, b) H atoms are omitted for clarity. Color codes: V (green), K (magenta), N (blue), O (red), and C (gray). (a, c) Views along the *a* (left) and *b* (right) axis; (c) 4-connected K1 nodes (magenta), centroids of 4-connected μ_4-L nodes (gray), centroids of 2-connected $[VO_2]^+$ (green) and μ-H_2O (red) linkers. Selected distances (Å): V1−N1 2.1332(15), V1−O1 1.9108(12), V1−O2 1.9665(12), V1−O3 1.6211(13), V1−O4 1.6415(13), K1−N2 2.9035(15), K1^{i}−O2 2.7858(13), K1^{ii} −O3 2.9113(14), K1^{ii} −O4 3.2262(15), K1−O5 3.2262(15), K1^{iii} −O5 2.8036(15), K1−O6 2.7380(16), K1^{ii}···V1 3.6962(5), K1···K1^{iii} 4.9823(6). Symmetry codes: (i) −1 − *x*, −*y*, 1 − *z*; (ii) *x*, 0.5 − *y*, −0.5 + *z*; (iii) −1 − *x*, −0.5 + *y*, 1.5 − *z*; (iv) −*x*, −*y*, 1 − *z*.

by the N2 and μ-O2 atoms of μ_4-L [K1−N2 2.9035(15), K1^{i}−O2 2.7858(13) Å], the μ-O3 and μ-O4 oxido ligands [K1−O3^{ii} 2.9113(14), K1−O4^{ii} 3.2262(15) Å], two μ-O5 atoms of μ-H_2O molecules [K1−O5 2.7273(15), K1−O5^{iii} 2.8036(15) Å], and the O6 atom of the terminal H_2O moiety [K1−O6 2.7380(16) Å]. As a result, the K1 and V1 centers are assembled into helical 1D ribbons that are constructed from the cyclic $[V(\mu\text{-}O)_2(\mu\text{-}O_L)K_2(\mu\text{-}H_2O)]$ subunits (Figure 2b). These ribbons run along the *b* axis and have the pitch of 7.2879(7) Å, equal to the *b* unit cell dimension. The adjacent ribbons are further interlinked via the μ_4-L spacers generating an infinite double-layered 2D metal−organic network. The packing pattern of **2** along the *c* axis shows that the neighboring 2D layers are repeated every 9.0644(5) Å (shortest metal···metal distance), also being mutually interdigitated and held together by means of interlayer H-bonds [O6−H6B···O1^{iv} 2.968(2) Å] into a 3D supramolecular framework.

$[\{V(\mu\text{-}O)(\mu_3\text{-}O)\}_2(\mu_8\text{-}L)\{Cs_2(\mu\text{-}H_2O)_2(H_2O)_2\}]_n$ ***(3)***. In spite of some similarities with **1** and **2**, the cesium containing structure of **3** is significantly more complex due to the presence of nine-coordinate Cs1 atoms and their intricate binding with μ_8-L, μ-oxido (O4), μ_3-oxido (O3), and μ-H_2O (O5) ligands. In contrast to **1** and **2**, the N2 nitrogen of μ_8-L is not bound to the Cs1 atom, while its phenolate oxygen (O1) acts in a different μ_3-mode and bridges two Cs1 and one V1 atoms. Another distinct feature of **3** concerns the overall μ_8-L bridging mode of the oxaloyldihydrazone ligand that is simultaneously linked to six Cs1 and two V1 atoms with a $\{N_2O_4\}$ donor set. Hence, the $\{CsO_9\}$ coordination environment is occupied by a number of symmetry equivalent oxygen atoms, namely two μ_3-O1 and one μ-O2 atoms of μ_8-L [Cs1−O1 3.5111(18), Cs1−O1^{ii} 3.2422(17), Cs1−O2^{iii} 3.2571(16) Å], two μ_3-O3 and one μ-O4 oxido ligands [Cs1−O3^{ii} 3.0334(16), Cs1−O3^{iii} 3.0444(16), Cs1−O4 3.1524(16) Å], two μ-O5 atoms from bridging water molecules [Cs1−O5 3.366(2), Cs1−O5^{iv} 3.5272(19) Å], and the O6 atom of terminal H_2O ligand [Cs1−O6 3.1914(19) Å]. Besides, there are the Cs1···C1 [3.574(2) Å] and Cs1···C2 [3.487(2) Å] contacts that are shorter than the sum of the van der Waals radii of the Cs and C atoms [3.70 Å],[17] and comparable to Cs···C distances in other reported compounds.[15a,18] The multiple binding of the Cs1 nodes with $[(VO_2)_2(\mu_8\text{-}L)]^{2-}$ blocks gives rise to the formation of intricate 2D double layers $[(VO)_2(\mu_8\text{-}L)Cs_2]_n$ (Figure 3c), which are further held together via μ-H_2O pillars generating a very complex layer-pillared 3D framework (Figure 3b).

Topological Analysis. To get an insight into the intricate 2D and 3D metal−organic networks of **1** and **2**, we performed their topological analysis[19] following the concept of the simplified underlying net.[20] Thus, after omitting terminal water ligands and reducing the μ_4-L, $[VO_2]^+$, and μ-H_2O moieties to their centroids, the structure of **2** can be described as an underlying 2D net built from the 4-connected K1 and μ_4-L nodes (topologically equivalent), and the 2-connected $[VO_2]^+$ and μ-H_2O linkers (Figure 2c). The topological analysis of this network discloses a uninodal 4-connected net with the **kgm** [Shubnikov plane net (3.6.3.6)/kagome pattern] topology and the point symbol of $(3^2.6^2.7^2)$.[19,21] In spite of being not very common, a few examples of coordination polymers with the **kgm** topology have been reported.[22]

Following the above-mentioned strategy,[19,20] we also obtained an underlying network of **3** (Figure 3d) by contracting the μ_8-L, $[VO_2]^+$, and μ-H_2O ligands to their centroids and eliminating terminal water molecules. The resulting trinodal 4,7,8-connected net is composed of the 4-connected $[VO_2]^+$, 7-connected Cs1, and 8-connected μ_8-L nodes, as well as 2-connected μ-H_2O linkers. Its topological analysis[19] reveals a novel topology with the point symbol of

dx.doi.org/10.1021/ic400743h | *Inorg. Chem.* XXXX, XXX, XXX−XXX

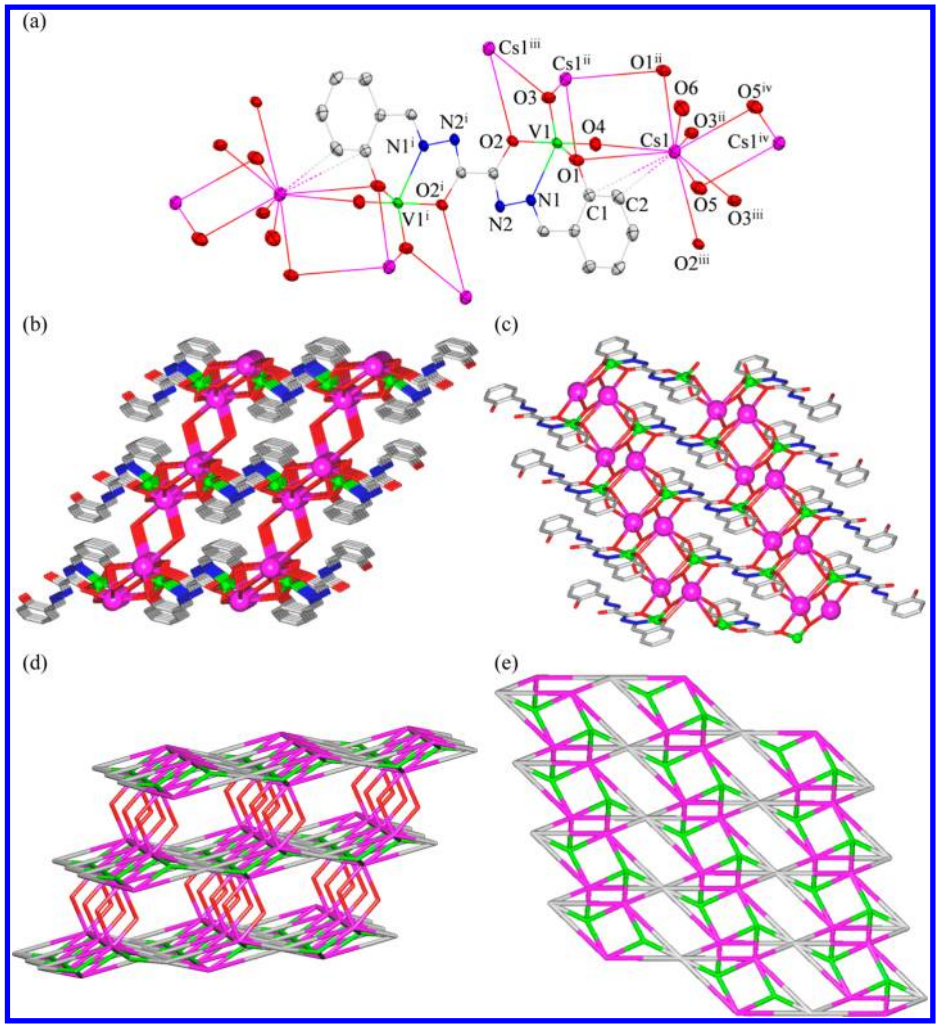

Figure 3. Structural fragments of **3** showing (a) ellipsoid plot (50% probability) with partial atom labeling scheme, (b) intricate layer-pillared 3D framework (view along the *a* axis) assembled from three $[(VO)_2(\mu_8\text{-L})Cs_2]_n$ double layers (side view) and μ-H_2O linkers, (c) front view of one 2D double layer, (d) topological representation of the underlying trinodal 4,7,8-connected 3D net with a new topology, which is composed of (e) topologically unique 2D metal−organic layers (front view of one layer). Further details: (a−c) all H atoms and terminal H_2O ligands (in b, c) are omitted for clarity. Color codes: V (green), Cs (magenta), N (blue), O (red), and C (gray); (d, e) 7-connected Cs nodes (magenta), centroids of 8-connected μ_8-L nodes (gray), centroids of 4-connected $[VO_2]^+$ nodes (green), centroids of 2-connected μ-H_2O linkers (red). Selected distances (Å): V1−N1 2.1360(19), V1−O1 1.9130(16), V1−O2 1.9955(16), V1−O3 1.6321(17), V1−O4 1.6326(17), Cs1−O1 3.5111(18), $Cs1^{ii}$−O1 3.2422(17), $Cs1^{iii}$ −O23.2571(16), $Cs1^{ii}$ −O3 3.0334(16), $Cs1^{iii}$ −O3 3.0444(16), Cs1−O4 3.1524(16), Cs1−O5 3.366(2), $Cs1^{iv}$−O5 3.5272(19), Cs1−O6 3.1914(19), Cs1···C1 3.574(2), Cs1···C2 3.487(2). Symmetry codes: (i) $-x, -y, 2-z$; (ii) $1-x, 1-y, 1-z$; (iii) $-1+x, y, z$; (iv) $2-x, -y, 1-z$.

$(3^3.4^3)_2(3^3.4^9.5^2.6^6.7)_2(3^6.4^8.5^4.6^7.7^2.8)$, wherein the notations $(3^3.4^3)$, $(3^3.4^9.5^2.6^6.7)$, and $(3^6.4^8.5^4.6^7.7^2.8)$ correspond to the $[VO_2]^+$, Cs1, and μ_8-L nodes, respectively. The undocumented character of the present topology has been confirmed by the search in different databases.[19,21] Interestingly, the 2D layers $[(VO)_2(\mu_8\text{-L})Cs_2]_n$ of **3** (Figure 3c) after simplification result in an underlying trinodal 4,6,8-connected net (Figure 3e) that also features a unique topology described by the point symbol of $(3^3.4^3)_2(3^3.4^9.5^2.6)_2(3^6.4^8.5^4.6^7.7^2.8)$. Hence, the present study contributes to the identification and classification of coordination polymers with new topologies.

Mild Oxidation of Cyclohexane. The compounds **1**−**3** were tested as precatalysts in the oxidation of cyclohexane by H_2O_2 at 50 °C in MeCN/H_2O medium (Scheme 3). The reactions were monitored by control sampling, typically after treatment by PPh_3[23] to reduce cyclohexyl hydroperoxide (primary intermediate product) to cyclohexanol, and then analyzed by gas chromatography determining the formation of

Scheme 3. Mild Oxidation of Cyclohexane

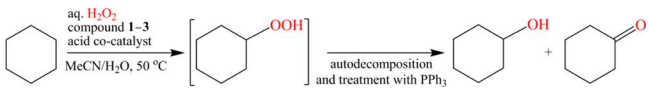

cyclohexanol and cyclohexanone as final products. The activity values discussed below concern the total yields, that is, sum of the molar % yields of the two final products (cyclohexanol and cyclohexanone) based on cyclohexane.

Although **1**−**3** are almost inactive as such (less than 0.5% total product yield), their catalytic performance is dramatically increased upon addition of a small amount of an acid promoter (cocatalyst). Thus, the total yield of cyclohexanol and cyclohexanone rose up to 19, 22, and 15% (Figure 4a) in the reactions catalyzed by **1**−**3**, respectively, in the presence of trifluoroacetic acid (TFA). Such a promoting behavior of an

dx.doi.org/10.1021/ic400743h | *Inorg. Chem.* XXXX, XXX, XXX−XXX

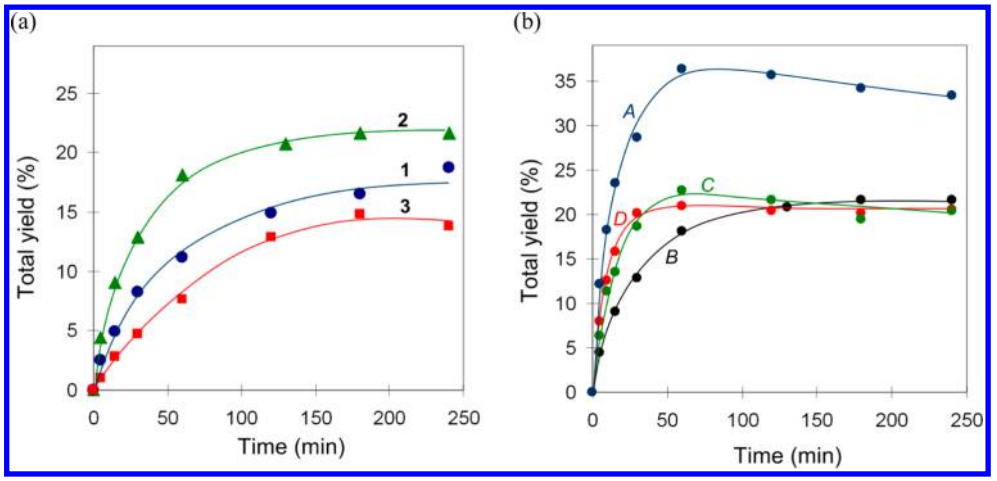

Figure 4. (a) Effect of the precatalyst type on the total yield of cyclohexanol and cyclohexanone in the oxidation of C_6H_{12} by H_2O_2 catalyzed by **1**–**3** (5×10^{-4} M) in the presence of TFA (5×10^{-3} M). (b) Effect of the acid promoter on the total yield of cyclohexanol and cyclohexanone in the oxidation of C_6H_{12} catalyzed by **2** (5×10^{-4} M) in the presence (5×10^{-3} M) of PCA (curve *A*), TFA (curve *B*), HCl (curve *C*), and H_2SO_4 (curve *D*). (a, b) General conditions: C_6H_{12} (0.46 M), H_2O_2 (2.2 M), 50 °C in MeCN.

acid cocatalyst is well-known for other V-catalyzed systems in oxidative transformation of alkanes.[11,23]

To understand whether the type of acid promoter has an influence on the oxidation of cyclohexane, we studied the effect of various acids using **2** as a precatalyst (Figure 4b). Hence, in the presence of HCl and H_2SO_4 the kinetic curves of products accumulation are very similar. Although the oxidation reactions proceed faster than those in the presence of TFA, the maximum product yields are the same (~22%) for all the three acids (Figure 4b, curves B–D). However, a different pattern is observed in the presence of 2-pyrazinecarboxylic acid (PCA), resulting in a significantly faster and more efficient reaction: 36% total yield and TON 340 after 1 h (Figure 4b, curve A). This behavior is consistent with the recognized application of PCA as a highly efficient cocatalyst in various V-catalyzed oxidative transformations.[9a,11a,b,d,23–25]

We also compared the activity of **1**–**3** (used in the 5×10^{-5} M concentration) in the presence of PCA (Figure 5). The kinetic curves of the product accumulation in cyclohexane oxidation are rather different for the three compounds, both in terms of the reaction rate and efficiency. The highest activity is exhibited by **3** resulting in the 32% total yield after 2 h with the corresponding TON of 2990, followed by **2** with the 24% total yield after 3 h and TON of 2220, and **1** with the 15% total yield after 4 h and TON of 1400 (Table 1, entries 1–3). Although the total yields drop off upon further decreasing the precatalyst concentration to 5×10^{-6} M, very high TONs of 5700, 5220, and 4400 can be achieved after 5 h in the cyclohexane oxidation catalyzed by **3**, **2**, and **1**, respectively (Table 1, entries 4–6). The analysis of the kinetic curves of the products accumulation in the oxidation of cyclohexane catalyzed by **2** taken in different concentrations (5×10^{-4} to 5×10^{-6} M) and in the presence of a constant PCA amount (Figure 6a) reveals a linear dependence of the maximum reaction rate (W_{max}) on the precatalyst concentration (Figure 6b).

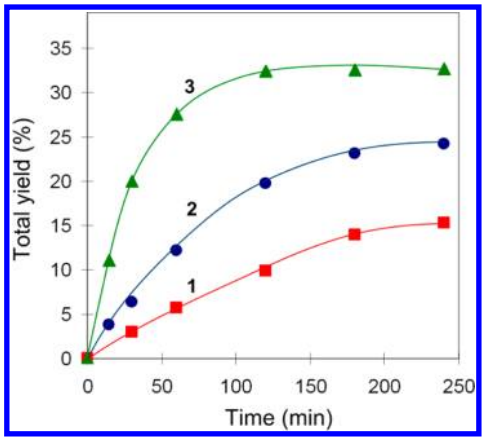

Figure 5. Effect of the precatalyst type on the total yield of cyclohexanol and cyclohexanone in the oxidation of C_6H_{12} (0.46 M) by H_2O_2 (2.2 M) catalyzed by **1**–**3** (5×10^{-5} M) in the presence of PCA (5×10^{-3} M), at 50 °C in MeCN.

In order to get some additional mechanistic information, we applied compounds **1**–**3** in combination with PCA for the oxidation of linear and branched cyclic alkanes, and the obtained results were compared with some related systems (Table 2).[11d,25] The oxidation of *n*-heptane proceeds with rather low regioselectivity [C(1):C(2):C(3):C(4) ≈ 1:(7–8):(7–9):(6–8)] and the secondary carbon atoms are oxidized preferably to the primary ones, although without particular selectivity to C(2), C(3), or C(4) position. In the oxidation of methylcyclohexane (MCH), the bond selectivity 1°:2°:3° parameters of 1:(6–7):(17–21) are very close for **1**–**3** and also comparable to those observed in other V-catalyzed oxidation reactions.[11d,25] The oxidation of *cis*- and *trans*-dimethylcyclohexane undergoes with some stereoselectivity and a partial inversion of the configuration, as attested by the *trans*/*cis* ratios in the 0.7–0.4 range between the formed tertiary alcohol isomers with the mutual *trans* and *cis* orientation of the methyl groups.

By analogy with other catalytic systems,[11d,25] the observed selectivity features indicate the involvement of hydroxyl radicals as oxidizing species in the present alkane oxidations by the **1**–**3**/PCA/H_2O_2 systems. Most likely $[(VO_2)_2(L)]^{2-}$ cores react with PCA to form active oxido-peroxido V-intermediates that participate in the generation of the HO$^{\bullet}$ radical from H_2O_2. The hydroxyl radical then abstracts an H atom from the alkane generating the alkyl radical R$^{\bullet}$, which further reacts with O_2 (e.g., from air) affording ROO$^{\bullet}$ and leading to the formation of alkyl hydroperoxide ROOH as a primary intermediate

dx.doi.org/10.1021/ic400743h | *Inorg. Chem.* XXXX, XXX, XXX–XXX

Table 1. Effect of the Precatalyst Type and its Concentration in the Oxidation of Cyclohexane by H_2O_2 in the Presence of PCA[a]

				product yield [%]			
entry	precatalyst	precatalyst concentration [M]	reaction time [min]	cyclohexanol	cyclohexanone	total[b]	TON[c]
1	**1**	5×10^{-5}	240	9.0	6.2	15.2	1400
2	**2**	5×10^{-5}	180	16.6	7.6	24.2	2220
3	**3**	5×10^{-5}	120	20.9	11.6	32.5	2990
4	**1**	5×10^{-6}	300	2.2	2.6	4.8	4400
5	**2**	5×10^{-6}	300	1.5	4.2	5.7	5220
6	**3**	5×10^{-6}	300	2.6	3.6	6.2	5700

[a]Reaction conditions: C_6H_{12} (0.46 M), PCA (5×10^{-3} M), H_2O_2 (50% aq., 2.2 M), MeCN (up to 5 mL total volume), 50 °C. [b]Moles of products (cyclohexanol + cyclohexanone)/100 mol of C_6H_{12}, determined by GC after the treatment with PPh_3. [c]Moles of products (cyclohexanol and cyclohexanone) per mol of precatalyst.

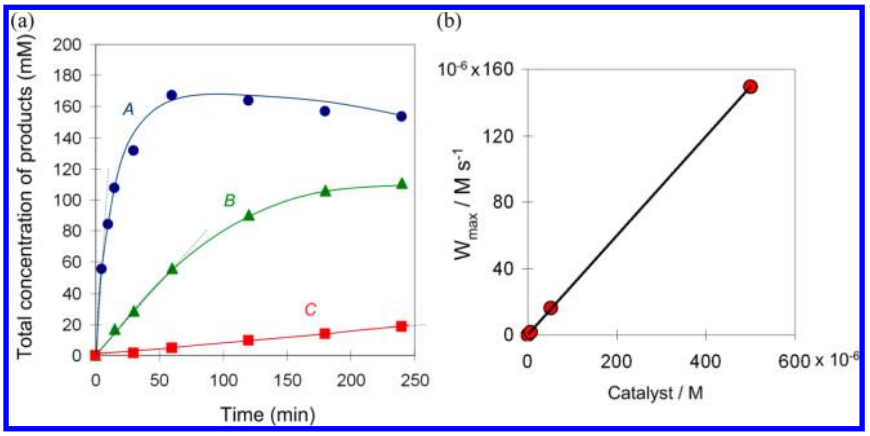

Figure 6. (a) Effect of the precatalyst amount. Accumulation of oxygenates (total concentration of cyclohexanol and cyclohexanone, mM) with time in the oxidation of C_6H_{12} (0.46 M) by H_2O_2 (2.2 M) in the presence of PCA (5×10^{-3} M) at 50 °C in MeCN catalyzed by **2**: 5×10^{-4} M (curve *A*), 5×10^{-5} M (curve *B*), 5×10^{-6} M (curve *C*). (b) Dependence of the maximum reaction rate W_{max} (M s^{-1}) on the concentration of **2** (data derived from part a).

Table 2. Selectivity Parameters in the Oxidation of Linear and Branched Cyclic Alkanes[a]

			stereoselectivity *trans*/*cis*	
catalytic system	regioselectivity (*n*-C_7H_{16}) C(1):C(2):C(3):C(4)	bond selectivity (MCH) 1°:2°:3°	*cis*-DMCH	*trans*-DMCH
1/PCA/H_2O_2	1:7:7:6	1:7:21	0.70	0.41
2/PCA/H_2O_2	1:8:8:7	1:6:18	0.56	0.41
3/PCA/H_2O_2	1:8:9:8	1:6:17	0.55	0.50
VO_3^-/PCA/H_2O_2[b]	1:9:7:7	1:6:18	0.75	0.80
[VO{N($C_2H_4O)_3$}]/PCA/H_2O_2[b]	1:6:6:5	1:4:10	0.70	0.75
hν/H_2O_2[b]	1:7:6:7		0.90	

[a]Abbreviations: MCH, methylcyclohexane; *cis*- and *trans*-DMCH, isomers of 1,2-dimethylcyclohexane. Reaction conditions: precatalyst **1**–**3** (5×10^{-4} M), $[PCA]_0$ = 0.005 M, $[substrate]_0$ = 0.46 M, $[H_2O_2]_0$ = 2.2 M (50% aq.), MeCN up to 5 mL total volume, 50 °C. All parameters were measured after reduction of the reaction mixtures with PPh_3 before GC analysis and calculated based on the ratios of isomeric alcohols. The calculated parameters were normalized taking into account the number of H atoms at each carbon atom. Parameters C(1):C(2):C(3):C(4) are relative reactivities of H atoms at C(1), C(2), C(3), and C(4) atoms of *n*-heptane. Parameters 1°:2°:3° are the relative normalized reactivities of the H atoms at primary, secondary, and tertiary carbon atoms of methylcyclohexane. Parameter *trans*/*cis* is determined as the ratio of the formed tertiary alcohol isomers with mutual *trans* and *cis* orientation of methyl groups. [b]Taken from reference 11d.

product.[9a,11,23–25] This rapidly decomposes (conceivably by V-catalyzed processes) to give alcohol and ketone as final products.[23–25] Alkyl hydroperoxides are common primary products in vanadium catalyzed alkane oxidation.[9a,11,25] Their generation in the present study was confirmed by performing the GC analyses of the reaction mixtures before and after the treatment with PPh_3, following a method developed by Shul'pin.[23] The involvement of $HO^•$ and $R^•$ radicals was further corroborated by a strong inhibiting effect on the formation of oxidation products, observed in the C_6H_{12} oxidation in the presence of O- or C-centered radical quenchers, either diphenylamine (Ph_2NH) or bromotrichloromethane ($CBrCl_3$), respectively.[12a] Hence, upon addition of Ph_2NH to the **2**/PCA/H_2O_2 system, the total yield of oxygenates dropped from 35 to 6% (conditions are those of Figure 6a, **2**: 5×10^{-4} M), while the introduction of $CBrCl_3$ resulted in the formation of cyclohexyl bromide as a main product (37% yield) instead of cyclohexanol and cyclohexanone.

To get further information on the vanadium speciation in the catalytic reaction mixtures, we have performed the ^{51}V NMR studies on the model aqueous (11 M H_2O) CD_3CN solutions containing **1** (5 mM). The ^{51}V NMR spectrum of **1** (δ −538) remains unchangeable upon addition of up to 10 equivalents of

dx.doi.org/10.1021/ic400743h | *Inorg. Chem.* XXXX, XXX, XXX–XXX

H_2O_2 (50 mM), while at high H_2O_2 concentrations (>0.5 M) a new signal at δ −719 (Figure S2, Supporting Information) is observed that corresponds to a di(peroxido) species such as $[VO(O_2)_2(CD_3CN)]^-$.[11d,26] The addition of PCA (20 mM, 4 equiv.) to the solution of **1** results in a negligible shift of the parent resonance from δ −538 to −536, along with some broadening of the signal (Figure S3, Supporting Information). The ^{1}H NMR spectrum of this solution reveals a shift of the PCA aromatic protons in comparison with "free" PCA, indicating that a considerable amount of PCA has been coordinated to vanadium, forming most likely the $[VO_2(pca)_2]^-$ or other di(oxido) derivatives containing both L(4−) and pca(1−) ligands. In fact, it was reported earlier[11d] that the $[VO_2(pca)_2]^-$ species in MeCN solution shows a ^{51}V resonance at δ −536. In the presence of 10 equiv. of PCA (50 mM), we have observed some widening of the resonance at δ −536 in the ^{51}V NMR spectrum, whereas two sets of proton signals corresponding to the coordinated and "free" PCA (~2:1) were found in the aromatic region of the ^{1}H NMR spectrum.

The addition of H_2O_2 (10 mM, 2 equiv.) to the solution of complex **1** (5 mM) containing PCA (20 mM, 4 equiv.) alters the ^{51}V spectrum (Figure S4, Supporting Information). Apart from the signal at δ −536, two new resonances at δ −552 and −566 appeared, which correspond to the two isomers (*trans*/*cis*) of the mono(peroxido) vanadium complex $[VO(O_2)(pca)_2]^-$.[25a,11d] The presence of these PCA containing species was also confirmed by ^{1}H MNR. Besides, there are two very weak ^{51}V resonances at δ −664 and −719 that correspond to the previously identified di(peroxido) species $[VO(O_2)_2(H_2O)]^-$ and $[VO(O_2)_2(CD_3CN)]^-$.[11d,25a] A higher excess of both PCA (50 mM, 10 equiv.) and H_2O_2 (0.5 M) (Figure S5) led to the disappearance of the $[VO_2(pca)_2]^-$ signal (δ −536). However, the intensity of other signals increased, namely those assigned to the *cis* and *trans* isomers of the PCA containing (mono)peroxido vanadium species, as well as the above di(peroxido) species bearing H_2O and MeCN ligands.

The ESI-MS(−) study of a model MeCN/H_2O solution containing **1**, H_2O_2 (10 equiv.), and PCA (4 equiv.) showed the generation of various oxido-peroxido species, in accord with the detection of the following fragments: $[\{VO(O_2)\}_2L(Na)_2(pca)_2 + H]^-$ (m/z = 814, 25% relative intensity, pca = anionic form of PCA), $[\{VO(O_2)\}_2L(Na)_3(pca) - H]^-$ (m/z = 712, 55%), and $[VO(O_2)(pca)_2]^-$ (m/z = 345, 100%), the latter being a recognized intermediate in other vanadium catalyzed oxidations promoted by PCA.[9a,11b,d,24,25] The formation of resembling oxido-peroxido species was also observed in the **2**/PCA/H_2O_2 and **3**/PCA/H_2O_2 model solutions. Interestingly, the oxido-peroxido derivatives do not appear to form upon treatment of **1**−**3** with H_2O_2 (10 equiv.) in the absence of PCA, as attested by the detection of $[(VO_2)L + 2H^+]^-$ (m/z = 407, 100% relative intensity) as major fragments in the corresponding ESI-MS(−) spectra. This fact apparently explains the inactivity of **1**−**3** in the absence of the PCA promoter. All these observations also testify that **1**−**3** are not intact in the course of alkane oxidations and act as homogeneous precatalysts, which furnish various oxido-peroxido V/M intermediates responsible for the generation of HO$^\bullet$ radicals as active oxidizing species.

CONCLUSIONS

In the present study, we synthesized and fully characterized three novel heterometallic vanadium(V)-alkali metal coordination polymers **1**−**3** composed of the $[(VO_2)_2(\mu_{4/8}\text{-L})]^{2-}$ cores and $[M_2(\mu\text{-}H_2O)_2(H_2O)_2]^{2+}$ moieties. The type of the alkali metal ion plays a key role in defining the complexity of the obtained coordination networks, which span from the Na-driven ladder-like 1D chains in **1** to K-driven double 2D layers in **2**, and Cs-driven layer-pillared 3D framework in **3**. This set of compounds represents an example of periodicity when the coordination number of the alkali metal [Na (5) < K (7) < Cs (9)] increases with its ionic radius, also with a concomitant growth of the network dimensionality [Na (1D) < K (2D) < Cs (3D)]. The work also contributes to the identification and classification of metal−organic materials with new topologies.[20] In particular, the structure of **3** features a trinodal 4,7,8-connected underlying net with a hitherto undocumented topology, whereas the structure of **2** shows a uninodal 4-connected underlying net with a rare **kgm** topology.

In addition, the compounds **1**−**3** represent rare examples of aqua-soluble coordination polymers that can be used as precatalysts in oxidation catalysis. In fact, **1**−**3** act as highly active catalyst precursors for the mild oxidation of cyclohexane, by aqueous H_2O_2 in MeCN/H_2O medium, to cyclohexanol and cyclohexanone. This transformation also requires the presence of an acid promoter that dramatically increases the rate of cyclohexane oxidation. The effect of different acid promoters (HCl, H_2SO_4, TFA, or PCA) has been studied, revealing the highest activity of 2-pyrazinecarboxylic acid. In spite of the presence of the resembling $[(VO_2)_2(\mu_{4/8}\text{-L})]^{2-}$ cores in **1**−**3**, their relative efficiencies depend on the reaction parameters, such as the type of acid promoter and the precatalyst concentration. Interestingly, under optimized conditions, the activity of **1**−**3** in the presence of PCA follows the trend **1** < **2** < **3** that can be explained by the different degrees of stabilization that the alkali metal ions provide to intermediate V-species. In fact, alkali metal aqua moieties are known to stabilize various oxido-peroxido complexes of vanadium.[7,27] The best total yields (based on substrate) of cyclohexanol and cyclohexanone up to 36% and turnover numbers (TONs) up to 5700 were shown by the **3**/PCA catalytic system.

In summary, the present work provides a contribution toward (i) widening the growing family of heterometallic vanadium-containing coordination polymers driven by alkali metals, (ii) identifying new structural and topological types of such materials, and (iii) applying them in oxidation catalysis. We believe future research should focus on the exploration of both synthetic and catalytic directions, namely by employing other types of vanadium building blocks and by broadening the substrate versatility of oxidative transformations.

EXPERIMENTAL SECTION

Materials and General Methods. All synthetic work was performed in air. All chemicals were obtained from commercial sources and used as received. Bis(salicylaldehyde)-oxaloyldihydrazone (H_4L) has been prepared by modification of a previously reported method.[6b] C, H, and N elemental analyses were carried out by the Microanalytical Service of the Instituto Superior Técnico. Infrared spectra (4000−400 cm^{-1}) were recorded on a BIO-RAD FTS 3000 MX instrument in KBr pellets (wavenumbers are in cm^{-1}. Abbreviations: vs, very strong; s, strong; m, medium; w, weak; br, broad; sh, shoulder). ^{1}H NMR spectra were recorded at ambient temperature on a Bruker Avance II 300 (UltraShield Magnet) spectrometer operating at 300.130 MHz. The chemical shifts (δ) are

dx.doi.org/10.1021/ic400743h | Inorg. Chem. XXXX, XXX, XXX−XXX

reported in ppm using tetramethylsilane as the internal reference (abbreviations: s, singlet; m, multiplet). ^{51}V NMR spectra were measured on a Bruker 400 (UltraShield Magnet) spectrometer at ambient temperature in aqueous CD_3CN. The vanadium chemical shifts are quoted relative to the external $VOCl_3$. A typical ^{51}V spectrum for a 5 mM solution of **1**−**3** was obtained from the accumulation of 10000 transients with a 900 ppm spectral window, at about 10 scans per second. An exponential line broadening up to 200 Hz was applied before Fourier transformation. UV−vis spectra of 10^{-4} M solutions of **1**−**3** in DMF were recorded on a Perkin-Elmer Lambda 35 instrument. ESI−MS(±) spectra were run on a 500-MS LC Ion Trap instrument (Varian Inc.) equipped with an electrospray (ESI) ion source, using ca. 10^{-3} M solutions of **1**−**3** in water or acetonitrile. Thermal analyses were performed with a Perkin-Elmer STA 6000 instrument. The crystalline samples were heated under N_2 atmosphere at the rate of 10 °C min^{-1} in the 30−950 °C temperature range. Gas chromatography (GC) analyses were performed on a Fisons Instruments GC 8000 series gas chromatograph with FID (He as carrier gas) and a capillary column BP20 (SGE) 30 m × 0.22 mm × 25 μm, using the Jasco-Borwin v. 1.50 software.

General Synthetic Procedure for 1−3. In a round-bottom flask (50 mL), H_4L (41 mg, 0.125 mmol) was mixed with ethanol (20 mL) under constant stirring. To that stirred suspension $[VO(acac)_2]$ (66 mg, 0.25 mmol) was added. The obtained mixture was refluxed for 2 h resulting, after cooling to room temperature (~25 °C), in a brown clear solution. To this solution an aqueous solution (10 mL) of alkali metal carbonate [Na_2CO_3 (27 mg, 0.25 mmol) for **1**; K_2CO_3 (35 mg, 0.25 mmol) for **2**; or Cs_2CO_3 (81 mg, 0.25 mmol) for **3**] was added, causing the immediate formation of a yellow precipitate. It was allowed to settle for about 1 h, then filtered, washed with ethanol, and dried over fused $CaCl_2$ to furnish compounds **1**, **2**, and **3** as yellow solids in 72, 70, and 76% yields based on H_4L, respectively. The X-ray quality single crystals of **1**−**3** were grown by a slow evaporation of their H_2O/DMF solutions (3:2, v/v), in air at room temperature.

$[(VO_2)_2(\mu_4\text{-}L)\{Na_2(\mu\text{-}H_2O)_2(H_2O)_2\}]_n$ ***(1)***. Soluble in H_2O ($S_{25°C} \approx 7$ mg mL^{-1}) and DMSO, slightly soluble in DMF and MeCN. Found: C, 31.35; H, 3.07; N, 8.93. $C_{16}H_{18}N_4Na_2O_{12}V_2$ (MW 606.2) requires C, 31.70; H, 2.99; N, 9.24. IR (KBr): 3435 (vs br) $\nu(H_2O)$, 1607 (vs) ν(C═O), 1547 (s) ν(C═N), 1472 (w), 1441 (w), 1372 (m), 1296 (s), 1272 (s), 1212 (w), 1149 (w), 915 (vs br) ν(V═O), 813 (w), 749 (s), 618 (w), 572 (w), and 462 (m) cm^{-1}. ^{1}H NMR (300 MHz, D_2O, Me_4Si), δ: 6.86−6.98 (m, 4H, Ar−H), 7.44−7.60 (m, 4H, Ar−H), 8.88 (s, 2H, C(H)═N). ^{51}V NMR (105 MHz, CD_3CN, $VOCl_3$), δ: −538. UV−vis (DMF): λ_{max}, nm (ε, L mol^{-1} cm^{-1}): 412 (12500), 324 (20500). ESI−MS(±) (H_2O), selected fragments with relative abundance >10%; MS(+) *m*/*z*: 690 (10%) $[(VO_2)_2(L)Na_2(H_2O)_4 + VO_2]^+$, 625 (30%) $[(VO_2)_2(L)Na_2(H_2O)_4 + H_2O + H]^+$, 557 (100%) $[(VO_2)_2(L)Na_2 + Na]^+$. MS(−) *m*/*z*: 511 (90%) $[(VO_2)_2(L)Na]^-$, 489 (60%) $[(VO_2)_2(L) + H]^-$, 244 (100%) $[(VO_2)_2(L)]^{2-}$.

$[\{V(\mu\text{-}O)_2\}_2(\mu_4\text{-}L)\{K_2(\mu\text{-}H_2O)_2(H_2O)_2\}]_n$ ***(2)***. Soluble in H_2O ($S_{25\ °C} \approx 5$ mg mL^{-1}) and DMSO, slightly soluble in DMF and MeCN. Found: C, 30.16; H, 2.55; N, 8.43. $C_{16}H_{18}K_2N_4O_{12}V_2$ (MW 638.4) requires C, 30.10; H, 2.84; N, 8.78. IR (KBr): 3442 (vs br) $\nu(H_2O)$, 1608 (vs) ν(C═O), 1548 (s) ν(C═N), 1475 (m), 1442 (w), 1371 (m), 1293 (m), 1270 (s), 1213 (m), 1154 (m), 1127 (w), 1030 (w), 913 (vs br) ν(V═O), 875 (sh), 814 (w), 749 (s), 621 (w), 575 (m), 518 (w), and 459 (m) cm^{-1}. ^{1}H NMR (300 MHz, D_2O, Me_4Si), δ: 6.86−6.98 (m, 4H, Ar−H), 7.44−7.61 (m, 4H, Ar−H), 8.89 (s, 2H, C(H)═N). ^{51}V NMR (105 MHz, CD_3CN, $VOCl_3$), δ −538. UV−vis (DMF), λ_{max}, nm (ε, L mol^{-1} cm^{-1}): 409 (3600), 324 (6400). ESI−MS(±) (H_2O), selected fragments with relative abundance >10%, MS(+) *m*/*z*: 686 (30%) $[(VO_2)_2(L)K_2(H_2O)_2 + VO_2]^+$, 660 (20%) $[(VO_2)_2(L)\text{-}K_2(H_2O)_3 + K]^+$, 604 (100%) $[(VO_2)_2(L)K_2(H_2O)_2 + H]^+$, 485 (20%) $[(VO_2)(L)K_2 + 2H]^+$. MS(−) *m*/*z*: 527 (85%) $[(VO_2)_2(L)\text{-}K]^-$, 489 (30%) $[(VO_2)_2(L) + H]^-$, 244 (100%) $[(VO_2)_2(L)]^{2-}$.

$[\{V(\mu\text{-}O)(\mu_3\text{-}O)\}_2(\mu_8\text{-}L)\{Cs_2(\mu\text{-}H_2O)_2(H_2O)_2\}]_n$ ***(3)***. Soluble in H_2O ($S_{25°C} \approx 4$ mg mL^{-1}) and DMSO, slightly soluble in DMF and MeCN. Found: C, 22.90; H, 2.00; N, 6.46. $C_{16}H_{18}Cs_2N_4O_{12}V_2$ (MW 826.0) requires C, 23.26; H, 2.20; N, 6.78. IR (KBr): 3433 (vs br) $\nu(H_2O)$, 1608 (vs) ν(C═O), 1547 (s) ν(C═N), 1523 (m), 1474 (m), 1443 (w), 1369 (m), 1291 (s), 1268 (s), 1211 (w), 1154 (w), 1129 (w), 1029 (w), 921 (vs br) ν(V═O), 872 (sh), 810 (w), 754 (s), 678 (w), 622 (w), 575 (m), and 459 (m) cm^{-1}. ^{1}H NMR (300 MHz, D_2O, Me_4Si), δ: 6.92−6.97 (m, 4H, Ar−H), 7.51−7.62 (m, 4H, Ar−H), 8.91 (s, 2H, C(H)═N). ^{51}V NMR (105 MHz, CD_3CN, $VOCl_3$), δ: −538. UV−vis (DMF) λ_{max}, nm (ε, L mol^{-1} cm^{-1}): 414 (15500), 325 (21300). ESI−MS(±) (H_2O), selected fragments with relative abundance >1%, MS(+): 886 (1%) $[(VO_2)_2(L)Cs_2 + Cs]^+$, 755 (1%) $[(VO_2)_2(L)Cs_2 + H]^+$, 133 (100%) $[Cs]^+$. MS(−) *m*/*z*: 621 (100%) $[(VO_2)_2(L)Cs]^-$, 244 (100%) $[(VO_2)_2(L)]^{2-}$.

X-ray Crystal Structure Determinations. The X-ray diffraction data of **1**−**3** were collected using a Bruker AXS-KAPPA APEX II diffractometer with graphite monochromated Mo Kα radiation. Data were collected using omega scans of 0.5° per frame, and a full sphere of data was obtained. Cell parameters were retrieved using Bruker SMART software and refined using Bruker SAINT on all the observed reflections.[28] Absorption corrections were applied using SADABS.[28] Structures were solved by direct methods using the SHELXS-97[29] or SIR97[30] programs and refined with SHELXL-97.[29] Calculations were performed with the WinGX System-Version 1.80.03.[31] All hydrogen atoms were inserted in calculated positions except those of coordinated water molecules; they were located from the final Fourier difference map, their coordinates were blocked during the refinement process, and the isotropic thermal parameters were set at 1.5 times the average thermal parameter of the belonging oxygen atoms. Crystal data and details of data collection for **1**−**3** are reported in Table 3.

Table 3. Crystal Data and Structure Refinement Details for Compounds 1−3

	1	2	3
empirical formula	$C_8H_9N_2NaO_6V$	$C_8H_9KN_2O_6V$	$C_8H_9CsN_2O_6V$
Fw	303.10	319.21	412.90
T (K)	150(2)	150(2)	150(2)
λ (Å)	0.71069	0.71069	0.71069
crystal system	Triclinic	Monoclinic	Triclinic
space group	*P*-1	$P2_1/c$	*P*-1
a (Å)	7.8121(4)	8.9859(4)	7.4312(2)
b (Å)	8.5243(4)	7.2879(4)	9.2421(3)
c (Å)	9.0869(6)	17.9664(7)	10.1449(3)
α (deg)	84.285(2)		64.3800(10)
β (deg)	70.705(2)	91.315(2)	83.907(2)
γ (deg)	80.472(1)		77.9490(10)
V (Å^3)	562.60(5)	1176.28(9)	614.30(3)
Z	2	4	2
ρ_{calcd} (g/cm^3)	1.789	1.803	2.233
μ(Mo Kα) (mm^{-1})	0.941	1.218	3.748
no. of collected reflns	5752	9258	11110
no. of unique reflns	2545	2593	2229
R_{int}	0.0336	0.0322	0.0261
Final *R*1[a], *wR*2[b] ($I \geq 2\sigma$)	0.0350, 0.0943	0.0263, 0.0689	0.0162, 0.0418
GOF on F^2	1.145	1.049	0.977

[a] $R1 = \Sigma||F_o| - |F_c||/\Sigma|F_o|$. [b] $wR2 = [\Sigma[w(F_o^2 - F_c^2)^2]/\Sigma[w(F_o^2)^2]]^{1/2}$

Alkane Oxidation Studies. The alkane oxidations were typically carried out in air in thermostatted (50 °C) Pyrex cylindrical vessels with vigorous stirring and using MeCN as solvent (up to 5.0 mL total volume). Typically, precatalyst **1**−**3** was introduced into the reaction mixture as a stock solution in acetonitrile (1.25×10^{-3} M). Then, an acid promoter (0.025 mmol, optional) was added either as solid (PCA) or stock solution in MeCN (TFA: 0.44 M. H_2SO_4: 0.355 M. HCl: 1.2 M). The substrate, typically cyclohexane (0.25 mL, 2.3 mmol), was introduced and the reaction started upon addition of hydrogen peroxide (50% in H_2O, 0.68 mL, 11 mmol) in one portion. The final concentrations of the reactants in the reaction mixture were

dx.doi.org/10.1021/ic400743h | Inorg. Chem. XXXX, XXX, XXX−XXX

as follows: precatalyst **1**–**3** ($5 \times 10^{-4} - 5 \times 10^{-6}$ M), acid promoter (5×10^{-3} M), substrate (0.46 M), and H_2O_2 (2.2 M). The oxidation reactions were monitored by withdrawing small aliquots after different periods of time, which were then cooled and treated with PPh_3 (for reduction of remaining H_2O_2 and alkyl hydroperoxides[23] that are formed as major primary products in alkane oxidations) followed by GC analysis. Attribution of peaks was made by comparison with the chromatograms of authentic samples. Nitromethane (0.05 mL) was used as GC internal standard.

■ ASSOCIATED CONTENT

Supporting Information

Figures S1–S5 with selected ^{51}V NMR spectra, crystallographic files in CIF format for compounds **1**–**3** (CCDC 927412-927414). This material is available free of charge via the Internet at http://pubs.acs.org.

■ AUTHOR INFORMATION

Corresponding Author

*Fax: +351 218464455. E-mail: kirillov@ist.utl.pt, pombeiro@ist.utl.pt, fatima.guedes@ist.utl.pt.

Notes

The authors declare no competing financial interest.

■ ACKNOWLEDGMENTS

This work was supported by the Foundation for Science and Technology (FCT) (projects PTDC/QUI-QUI/121526/2010, PTDC/QUI-QUI/102150/2008, and PEst-OE/QUI/UI0100/2013), Portugal. We also thank Dr J. Lasri for assistance with some ^1H NMR measurements and Dr M. C. Oliveira for ESI-MS (IST-node of the RNEM/FCT).

■ REFERENCES

(1) For selected state-of-the-art books on coordination polymers, see the following: (a) Ortiz, O. L.; Ramírez, L. D. *Coordination Polymers and Metal Organic Frameworks: Properties, Types, and Applications*; Nova Science Publishers, Inc.: Hauppauge, NY, 2012. (b) *Metal-Organic Frameworks: Applications from Catalysis to Gas Storage*; Farrusseng, D., Ed.; Wiley: New York, 2011. (c) *Metal-Organic Frameworks: Design and Application*; MacGillivray, L. R., Ed.; Wiley: New York, 2010. (d) *Functional Metal-Organic Frameworks: Gas Storage, Separation, and Catalysis*; Schroder, M., Ed.; Springer: New York, 2010. (e) *Design and Construction of Coordination Polymers*; Hong, M.-C., Chen, L., Eds.; Wiley: New York, 2009. (f) Batten, S. R.; Turner, D. R.; Neville, S. M. *Coordination Polymers: Design, Analysis and Application*; RSC: London, 2009.

(2) For selected reviews, see the following: (a) Stock, N.; Biswas, S. *Chem. Rev.* **2012**, *112*, 933. (b) Paz, F. A. A.; Klinowski, J.; Vilela, S. M. F.; Tomé, J. P. C.; Cavaleiro, J. A. C.; Rocha, J. *Chem. Soc. Rev.* **2012**, *41*, 1088. (c) Janiak, C.; Vieth, J. K. *New J. Chem.* **2010**, *34*, 2366. (d) Fromm, K. M.; Sague, J. L.; Mirolo, L. *Macromol. Symp.* **2010**, *291–292*, 75.

(3) For selected recent examples of vanadium coordination polymers, see the following: (a) Khan, N. A.; Jhung, S. H. *Angew. Chem., Int. Ed.* **2012**, *51*, 1198. (b) Olshansky, J. H.; Thanh, T. T.; Hernandez, K. J.; Zeller, M.; Halasyamani, P. S.; Schrier, J.; Norquist, A. J. *Inorg. Chem.* **2012**, *51*, 11040. (c) Phan, A.; Czaja, A. U.; Gandara, F.; Knobler, C. B.; Yaghi, O. M. *Inorg. Chem.* **2011**, *50*, 7388. (d) Kanoo, P.; Ghosh, A. C.; Maji, T. K. *Inorg. Chem.* **2011**, *50*, 5145. (e) Khan, N. A.; Jun, J. W.; Jeong, J. H.; Jhung, S. H. *Chem. Commun.* **2011**, *47*, 1306. (f) Centrone, A.; Harada, T.; Speakman, S.; Hatton, T. A. *Small* **2010**, *6*, 1598.

(4) (a) Rehder, D. *Bioinorganic Vanadium Chemistry*; Wiley: Chichester, 2008. (b) Tracey, S.; Willsky, G. R.; Takeuchi, E. S. *Vanadium Chemistry, Biochemistry, Pharmacology and Practical Applications*; CRC Press: Boca Raton, 2007. (c) Kustin, K.; Pessoa, J. C.; Crans, D. C. (Eds.), *Vanadium: The Versatile Metal*, ACS Symp. Ser. 974; American Chemical Society: Washington DC, 2007. (d) Crans, D. C.; Smee, J. J.; Gaidamauskas, E.; Yang, L. *Chem. Rev.* **2004**, *104*, 849. (e) Crans, D. C.; Smee, J. J. In *Comprehensive Coordination Chemistry II*, 2nd ed.; McCleverty, T. A., Meyer, J., Eds.; Elsevier Pergamon: Oxford, U.K., 2004; Vol. *4*, pp 175–239.

(5) Zhang, X.-M.; You, X.-Z.; Wang, X. *Polyhedron* **1996**, *15*, 1793.

(6) (a) Kumar, A.; Borthakur, R.; Koch, A.; Chanu, O. B.; Choudhury, S.; Lemtur, A.; Lal, R. A. *J. Mol. Struct.* **2011**, *999*, 89. (b) Lal, R. A.; Choudhury, S.; Ahmed, A.; Chakraborty, M.; Borthakur, R.; Kumar, A. *J. Coord. Chem.* **2009**, *62*, 3864.

(7) See the Cambridge Structural Database (CSD, version 5.34, May 2013): Allen, F. H. *Acta Crystallogr.* **2002**, *B58*, 380.

(8) (a) Banerjee, D.; Parise, J. B. *Cryst. Growth Des.* **2011**, *11*, 44704. (b) Fromm, K. M. *Coord. Chem. Rev.* **2008**, *252*, 856.

(9) For selected reviews, see the following: (a) da Silva, J. A. L.; Fraústo da Silva, J. J. R.; Pombeiro, A. J. L. *Coord. Chem. Rev.* **2011**, *255*, 2232. (b) Maurya, M. R.; Kumar, A.; Pessoa, J. C. *Coord. Chem. Rev.* **2011**, *255*, 2315. (c) Mizuno, N.; Kamata, K. *Coord. Chem. Rev.* **2011**, *255*, 2358. (d) Conte, V.; Coletti, A.; Floris, B.; Licini, G.; Zonta, C. *Coord. Chem. Rev.* **2011**, *255*, 2165.

(10) (a) Kirillova, M. V.; Kuznetsov, M. L.; Reis, P. M.; da Silva, J. A. L.; Fraústo da Silva, J. J. R.; Pombeiro, A. J. L. *J. Am. Chem. Soc.* **2007**, *129*, 10531. (b) Kirillova, M. V.; Kuznetsov, M. L.; da Silva, J. A. L.; Guedes da Silva, M. F. C.; Fraústo da Silva, J. J. R.; Pombeiro, A. J. L. *Chem.—Eur. J.* **2008**, *14*, 1828. (c) Kirillova, M. V.; da Silva, J. A. L.; Fraústo da Silva, J. J. R.; Palavra, A. F.; Pombeiro, A. J. L. *Adv. Synth. Catal.* **2007**, *349*, 1765. (d) Kirillova, M. V.; Kirillov, A. M.; Reis, P. M.; Silva, J. A. L.; Fraústo da Silva, J. J. R.; Pombeiro, A. J. L. *J. Catal.* **2007**, *248*, 130. (e) Reis, P. M.; Silva, J. A. L.; Palavra, A. F.; Fraústo da Silva, J. J. R.; Pombeiro, A. J. L. *J. Catal.* **2005**, *235*, 333. (f) Reis, P. M.; Silva, J. A. L.; Fraústo da Silva, J. J. R.; Pombeiro, A. J. L. *J. Chem. Soc., Chem. Commun.* **2000**, 1845. (g) Reis, P. M.; Silva, J. A. L.; Palavra, A. F.; Fraústo da Silva, J. J. R.; Kitamura, T.; Fujiwara, Y.; Pombeiro, A. J. L. *Angew. Chem., Int. Ed.* **2003**, *42*, 821.

(11) (a) Sutradhar, M.; Kirillova, M. V.; Guedes da Silva, M. F. C.; Martins, L. M. D. R. S.; Pombeiro, A. J. L. *Inorg. Chem.* **2012**, *51*, 11229. (b) Kirillova, M. V.; Kuznetsov, M. L.; Kozlov, Y. N.; Shul'pina, L. S.; Kitaygorodskiy, A.; Pombeiro, A. J. L.; Shul'pin, G. B. *ACS Catal.* **2011**, *1*, 1511. (c) Silva, T. F. S.; Luzyanin, K. V.; Kirillova, M. V.; Guedes da Silva, M. F. C.; Martins, L. M. D. R. S.; Pombeiro, A. J. L. *Adv. Synth. Catal.* **2010**, *352*, 171. (d) Kirillova, M. V.; Kuznetsov, M. L.; Romakh, V. B.; Shul'pina, L. S.; Fraústo da Silva, J. J. R.; Pombeiro, A. J. L.; Shul'pin, G. B. *J. Catal.* **2009**, *267*, 140. (e) Silva, T. F. S.; Alegria, E. C. B. A.; Martins, L. M. D. R. S.; Pombeiro, A. J. L. *Adv. Synth. Cat.* **2008**, *350*, 706. (f) Silva, T. F. S.; Mac Leod, T. C. O.; Martins, L. M. D. R. S.; Guedes da Silva, M. F. C.; Schiavon, M. A.; Pombeiro, A. J. L. *J. Mol. Cat. A: Chem.* **2013**, *367*, 52.

(12) (a) Kirillov, A. M.; Kirillova, M. V.; Pombeiro, A. J. L. *Coord. Chem. Rev.* **2012**, *256*, 2741. (b) Kirillova, M. V.; Kirillov, A. M.; Martins, A. N. C.; Graiff, C.; Tiripicchio, A.; Pombeiro, A. J. L. *Inorg. Chem.* **2012**, *51*, 5224. (c) Kirillov, A. M.; Coelho, J. A. S.; Kirillova, M. V.; Guedes da Silva, M. F. C.; Nesterov, D. S.; Gruenwald, K. R.; Haukka, M.; Pombeiro, A. J. L. *Inorg. Chem.* **2010**, *49*, 6390.

(13) (a) Gasnier, A.; Barbe, J.-M.; Bucher, C.; Duboc, C.; Moutet, J.-C.; Saint-Aman, E.; Terech, P.; Royal, G. *Inorg. Chem.* **2010**, *49*, 2592. (b) Folch, B.; Larionova, J.; Guari, Y.; Molvinger, K.; Luna, C.; Sangregorio, C.; Innocenti, C.; Caneschi, A.; Guerin, C. *Phys. Chem. Chem. Phys.* **2010**, *12*, 12760. (c) Friese, V. A.; Kurth, D. G. *Coord. Chem. Rev.* **2008**, *252*, 199.

(14) (a) Amin, S. S.; Cryer, K.; Zhang, B.; Dutta, S. K.; Eaton, S. S.; Anderson, O. P.; Miller, S. M.; Reul, B. A.; Brichard, S. M.; Crans, D. C. *Inorg. Chem.* **2000**, *39*, 406. (b) Tsuchida, E.; Yamamoto, K.; Oyaizu, K. In *Bioinorganic Catalysis*; Reedijk, J., Bouwman, E., Eds.; CRC Press: Boca Raton, FL, 1999; Ch. 15. (c) Nakamoto, K. *Infrared and Raman Spectra of Inorganic and Coordination Compounds*, 5th ed.; Wiley: New York, 1997.

(15) (a) Maurya, M. R.; Khan, A. A.; Azam, A.; Ranjan, S.; Mondal, N.; Kumar, A.; Avecilla, F.; Pessoa, J. C. *Dalton Trans.* **2010**, *39*, 1345.

(b) Ranford, J. D.; Vittal, J. J.; Wang, Y. M. *Inorg. Chem.* **1998**, *37*, 1226.
(16) (a) Horcajada, P.; Gref, R.; Baati, T.; Allan, P. K.; Maurin, G.; Couvreur, P.; Férey, G.; Morris, R. E.; Serre, C. *Chem. Rev.* **2012**, *112*, 1232. (b) McKinlay, A. C.; Morris, R. E.; Horcajada, P.; Férey, G.; Gref, R.; Couvreur, P.; Serre, C. *Angew. Chem., Int. Ed.* **2010**, *49*, 6260.
(17) Bondi, A. *J. Phys. Chem.* **1964**, *68*, 441.
(18) (a) Hanna, T. A.; Liu, L.; Angeles-Boza, A. M.; Kou, X.; Gutsche, C. D.; Ejsmont, K.; Watson, W. H.; Zakharov, L. N.; Incarvito, C. D.; Rheingold, A. L. *J. Am. Chem. Soc.* **2003**, *125*, 6228. (b) Rabe, G. W.; Liable-Sands, L. M.; Incarvito, C. D.; Lam, K.-C.; Rheingold, A. L. *Inorg. Chem.* **1999**, *38*, 4342.
(19) Blatov, V. A. *IUCr CompComm Newsletter* **2006**, *7*, 4.
(20) (a) Blatov, V. A.; Proserpio, D. M. In *Modern Methods of Crystal Structure Prediction*; Oganov, A. R., Ed.; Wiley: New York, 2010; pp 1−28. (b) Blatov, V. A.; O'Keeffe, M.; Proserpio, D. M. *CrystEngComm* **2010**, *12*, 44. (c) Alexandrov, E. V.; Blatov, V. A.; Kochetkova, A. V.; Proserpio, D. M. *CrystEngComm* **2011**, *13*, 3947. (d) O'Keeffe, M.; Yaghi, O. M. *Chem. Rev.* **2012**, *112*, 675.
(21) The Reticular Chemistry Structure Resource (RCSR) Database; O'Keeffe, M.; Peskov, M. A.; Ramsden, S. J.; Yaghi, O. M. *Acc. Chem. Res.* **2008**, *30*, 1782.
(22) (a) Liu, X.; Oh, M.; Lah, M. S. *Inorg. Chem.* **2011**, *50*, 5044. (b) Kondo, M.; Takashima, Y.; Seo, J.; Kitagawa, S.; Furukawa, S. *CrystEngComm* **2010**, *12*, 2350. (c) Li, C.-P.; Tian, Y.-L.; Guo, Y.-M. *Inorg. Chem. Commun.* **2008**, *11*, 1405.
(23) (a) Shul'pin, G. B. *C. R. Chim.* **2003**, *6*, 163. (b) Shul'pin, G. B. *J. Mol. Catal. A: Chem.* **2002**, *189*, 39. (c) Shul'pin, G. B. *Mini-Rev. Org. Chem.* **2009**, *6*, 95.
(24) Kirillov, A. M.; Shul'pin, G. B. *Coord. Chem. Rev.* **2013**, *257*, 732.
(25) (a) Shul'pin, G. B.; Kozlov, Y. N.; Nizova, G. V.; Süss-Fink, G.; Stanislas, S.; Kitaygorodskiy, A.; Kulikova, V. S. *J. Chem. Soc., Perkin Trans. 2* **2001**, 1351. (b) Kozlov, Y. N.; Romakh, V. B.; Kitaygorodskiy, A.; Buglyó, P.; Süss-Fink, G.; Shul'pin, G. B. *J. Phys. Chem. A* **2007**, *111*, 7736. (c) Süss-Fink, G.; Stanislas, S.; Shul'pin, G. B.; Nizova, G. V. *Appl. Organomet. Chem.* **2000**, *14*, 623. (d) Süss-Fink, G.; Stanislas, S.; Shul'pin, G. B.; Nizova, G. V.; Stoeckli-Evans, H.; Neels, A.; Bobillier, C.; Claude, S. *J. Chem. Soc., Dalton Trans.* **1999**, 3169. (e) Shul'pin, G. B.; Attanasio, D.; Suber, L. *J. Catal.* **1993**, *142*, 147.
(26) Slebodnick, C.; Pecoraro, V. L. *Inorg. Chim. Acta* **1998**, *283*, 37.
(27) (a) Sivak, M.; Sucha, V.; Kuchta, L.; Marek, J. *Polyhedron* **1999**, *18*, 93. (b) Fedorova, E. V.; Rybakov, V. B.; Senyavin, V. M.; Aslanov, L. A.; Anisimov, A. V. *Russ. J. Coord. Chem.* **2002**, *28*, 516. (c) Tatiersky, J.; Schwendt, P.; Marek, J.; Sivak, M. *New J. Chem.* **2004**, *28*, 127.
(28) Bruker, *APEX2 & SAINT*; AXS Inc.: Madison, WI, 2004.
(29) Sheldrick, G. M. *Acta Crystallogr.* **2008**, *A64*, 112.
(30) Altomare, A.; Burla, M. C.; Camalli, M. C.; Giacovazzo, C.; Guagliardi, A.; Moliterni, A. G. G.; Polidori, G.; Spagna, R. *J. Appl. Crystallogr.* **1999**, *32*, 115.
(31) Farrugia, L. J. *J. Appl. Crystallogr.* **1999**, *32*, 837.

dx.doi.org/10.1021/ic400743h | *Inorg. Chem.* XXXX, XXX, XXX−XXX